# MECHATRONIC CYBER PHYSICAL MEDICAL DEVICE FOR MONITORING LOWER EXTREMITY REHABILITATION: PROSPECTS AND CHALLENGES

SANGHERA, M. S.[1*] – SAINI, M.[1] – SACHDEV, I.[1] – GUPTA, H.[1]

[1] *Mechanical Engineering Department, Thapar Institute of Engineering and Technology, Punjab, India.*

**Corresponding author*
*e-mail: manjot9122002[at]gmail.com*

(Received 19th June 2024; revised 21st September 2024; accepted 29th September 2024)

**Abstract.** In this study a mechatronic cyber-physical medical device was designed with the objective of monitoring, aiding lower extremity rehabilitation and reports about the challenges encountered during the course of its development and evaluation. Device involved the integration of force-sensitive resistors (FSRs) embedded in an insole to measure plantar pressure distribution and an IMU-MPU6050 to monitor dorsiflexion and plantarflexion angles of the ankle. It is capable of providing real-time data to physiotherapists and assists in patient movement through direct current (DC) motors and Bowden cables. This paper highlights the anatomical and biomechanical parameters (range of motion (ROM) and load distribution) of the human foot and ankle, the limitations of conventional rehabilitation techniques (like lack of objective monitoring, cost and time constraints) and various innovative solutions like real time reporting of progress, historicization of patient's records etc. offered through the device developed by our team. Prototype so developed demonstrates significant potential for improving lower extremity rehabilitation and encourages data driven physiotherapeutic treatments besides some limitations identified in sensor accuracy and movement constraints. For the commercial use of the prototype, it is suggested that extensive clinical trials should be conducted with enhanced device mobility and integration of high throughput advance sensors.
**Keywords**: *lower extremity rehabilitation, cyber-physical system, mechatronics, plantar pressure, dorsiflexion, plantarflexion*

## Introduction

Lower extremity rehabilitation is a critical component in the recovery process for individuals who have experienced injuries, surgeries, or neurological impairments affecting their mobility. Traditional rehabilitation methods, while effective, often rely on manual techniques administered by physiotherapists, which can introduce variability in treatment outcomes due to differences in skill and experience among practitioners. This inconsistency highlights a need for more precise and standardized approaches in rehabilitation. The foot and ankle complex plays a crucial role in overall body mechanics and health. Improper rehabilitation of these structures can lead to a cascade of issues throughout the kinetic chain, potentially causing back, hip, and knee pain, as well as postural imbalances and reduced quality of life. The foot is the base of the lower quarter kinetic chain, thus if rehabilitation and treatment is not managed properly, an injury to the foot or ankle can ultimately cause secondary injuries elsewhere up the chain (Chinn and Hertel, 2010). Given the far-reaching implications of lower extremity injuries, the rehabilitation process is vital in restoring function and enabling patients to regain their active lifestyles. However, current rehabilitation approaches face several limitations. Chief among these is the lack of personalization in treatment plans. Traditional instruments often focus on specific aspects of rehabilitation, missing a

comprehensive view of a patient's overall functional status (Jette and Haley, 2005). Furthermore, the reliance on subjective assessments by healthcare professionals can introduce inconsistencies in evaluating and monitoring patient progress. Without objective means of tracking performance and response to interventions, optimizing treatment plans becomes challenging. A mechatronic cyber-physical medical device offers new possibilities for enhancing the effectiveness and efficiency of therapy. Representing a significant advancement in rehabilitation science. These systems have the potential to provide real-time, data-driven insights that can inform more personalized and adaptive treatment strategies (Feng et al., 2021). This paper reports the integration of a mechatronics-based Cyber-Physical System (CPS) for monitoring and aiding foot rehabilitation in real-time to address the limitations faced during conventional physiotherapeutic approaches. To achieve potentially improved outcomes, the said technology facilitates more data-driven and patient-centric rehabilitation processes. The subsequent sections of the paper will deliberate on the design, implementation, and preliminary results of our proposed prototype, as well as its implications for further improvement in lower extremity rehabilitation.

### *Anatomy of human foot*

The foot and ankle are essential for complex coordinated movements such as walking and maintaining an upright stance (*Figure 1*). The foot, located below the ankle joint, comprises a sophisticated anatomical structure of bones, joints, ligaments, muscles, and tendons. Specifically, the ankle joint, or tibiotalar joint, is formed by the talus bone and the recess created by the distal tibia and fibula. The foot consists of 26 bones, divided into tarsal, metatarsal, and phalanges, and is further categorized into the hindfoot, midfoot, and forefoot. Articular cartilage covers the bone surfaces at the joints, which are stabilized by joint capsules and ligaments. There are 29 muscles that facilitate the movement of the foot and ankle, attaching to bones via tendons.

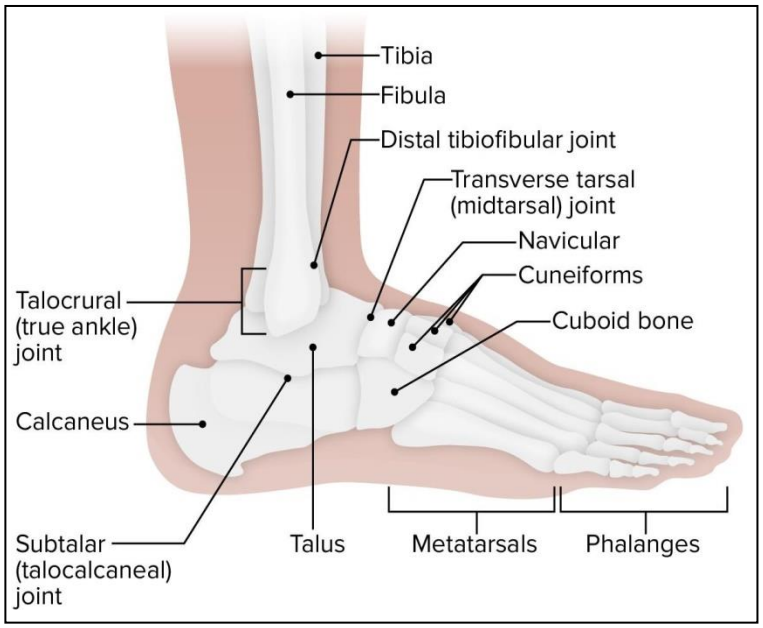


***Figure 1.*** *Lateral view of the ankle.*

*Subtalar Joint*: The subtalar joint, also known as the talocalcaneal joint, is a critical component of the foot's biomechanics. It is formed by the articulation between the talus and the calcaneus. This joint allows for inversion and eversion movements of the foot. The stability of the subtalar joint is maintained by several ligaments, including the interosseous talocalcaneal ligament, the lateral talocalcaneal ligament, and the anterior talocalcaneal ligament. Additionally, the calcaneofibular part of the lateral collateral ligament and the tibiocalcaneal ligament of the deltoid contribute to the joint's support.

*Tibiotalar Joint* (Talocrural Joint): The tibiotalar joint, or talocrural joint, is the main joint involved in dorsiflexion and plantarflexion of the foot. It is a hinge joint formed by the distal ends of the tibia and fibula, which create a mortise that accommodates the trochlea of the talus. This joint is stabilized by the medial and lateral collateral ligaments, and the syndesmosis of the tibia and fibula, which includes the anterior and posterior tibiofibular ligaments and the interosseous membrane.

*Inferior Tibiofibular Joint*: The inferior tibiofibular joint is a syndesmotic joint, rather than a synovial joint, connecting the distal tibia and fibula. This joint is stabilized by the anterior and posterior tibiofibular ligaments, as well as the interosseous ligament. Its primary function is to provide stability to the ankle joint, particularly during weight-bearing activities.

*Transverse Tarsal Joint*: The transverse tarsal joint, also known as Chopart's joint, consists of two joints: the talonavicular joint and the calcaneocuboid joint. It plays a significant role in the inversion and eversion movements of the foot. This joint functions in conjunction with the subtalar joint, sharing a common axis of motion and contributing to the complex movements necessary for walking and running.

Muscles of the Ankle: The ankle's movement is controlled by twelve extrinsic muscles divided into four compartments: (a) Anterior Compartment: Includes the tibialis anterior, extensor digitorum longus, extensor hallucis longus, and peroneus tertius. These muscles are primarily responsible for dorsiflexion and inversion of the foot; (b) Lateral Compartment: Contains the peroneus longus and peroneus brevis, which produce plantarflexion and eversion; (c) Posterior Compartment: Comprises the gastrocnemius, soleus, and plantaris, contributing to plantarflexion; and (d) Deep Posterior Compartment: Includes the tibialis posterior, flexor digitorum longus, and flexor hallucis longus, which are involved in plantarflexion and inversion. Injuries or conditions affecting the foot and ankle, such as acute or chronic repetitive injuries, and degenerative or inflammatory arthropathies, often lead to medical consultations. Without proper treatment, these issues can cause long-term disability (Ficke and Byerly, 2019).

### *Functions of human foot*

The key movement of the ankle joint complex are plantar- and dorsiflexion, occurring in the sagittal plane; ab-/adduction occurring in the transverse plane and inversion-eversion, occurring in the frontal plane (*Figure 2*). (1) Dorsiflexion and Plantarflexion: Dorsiflexion and plantarflexion occur primarily in the sagittal plane at the ankle joint. Dorsiflexion refers to the upward movement of the foot, decreasing the angle between the dorsum (top) of the foot and the leg. Plantarflexion is the downward movement, increasing this angle. The normal range of motion for dorsiflexion is about 10-20 degrees, while plantarflexion ranges from 40-55 degrees. (2) Inversion and Eversion: Inversion and eversion are movements in the frontal plane. Inversion involves tilting the sole of the foot towards the midline, whereas eversion tilts it away from the

midline. The subtalar joint plays a significant role in these movements. The typical range of motion for inversion is approximately 20 degrees, and for eversion, it is around 10 degrees. (3) Weight-Bearing and Stability: The foot, particularly the first and second rays, is essential for weight-bearing. The first and second metatarsophalangeal joints (MTP joints) contribute significantly to balance, weight distribution, and gait. Muscles and tendons are primarily responsible for the coordinated movements of the osseous structures of the foot and ankle, but they also lend stability to the osseous and ligamentous anatomy.

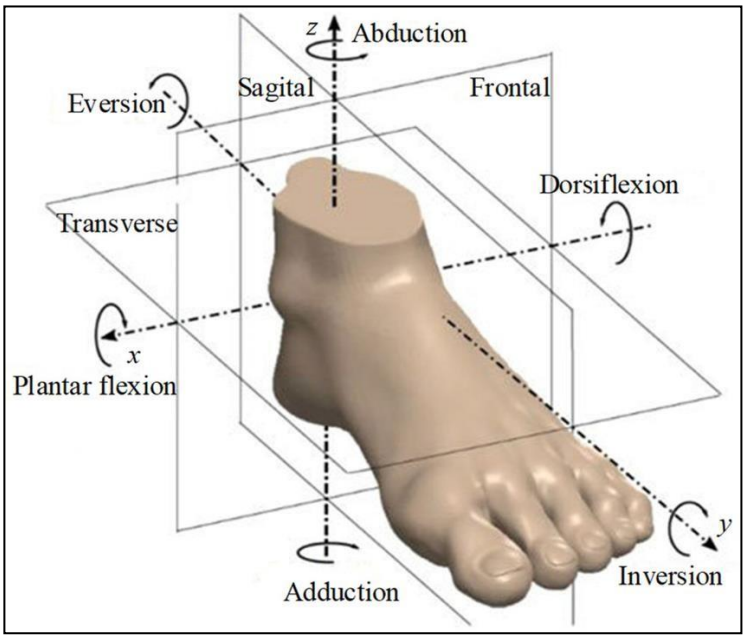


***Figure 2.*** *The movements of the ankle joint.*

### *Biomechanics of human foot*

### *Gait cycle of human foot*

The complex anatomy of the foot and ankle, together with the remainder of the lower limb, efficiently supports body weight and provides locomotion. The foot functions as a platform for stance, a shock absorber during impact, and a lever to propel the body forward during stepping (Ficke and Byerly, 2019). As the body moves forward, one limb act as source of support while the other limb advances itself to a new support site. Then the limbs reverse their roles. This series of events is repeated by each limb with reciprocal timing until the person's destination is reached. A single sequence of these functions by one limb is called a gait cycle (GC). Normal persons initiate floor contact with their heel (i.e.,heel strike).Each gait cycle is divided into two periods, stance and swing also known as gait phases (as in *Figure 1*). Stance is the term used to designate the entire period during which the foot is on the ground. Stance begins with initial contact. The word swing applies to the time the foot is in the air for limb advancement. Swing begins as the foot is lifted from the floor (toe-off) (Kharb et al., 2011). Gait consists of repetitive cycles of the stance phase, when the foot is on the ground (foot strike, mid-stance, and terminal stance), and the swing phase, when the foot is in the air (*Figure 3*). During walking foot strike, the foot is supinated, and the Chopart joint is locked, making the foot rigid when the heel first lands. The foot pronates and flattens

during mid-stance, coming into full contact with the surface. Terminal stance is characterized by propulsion via heel-off and toe-off. The Lisfranc joint allows slight dorsiflexion and plantarflexion. Force then transfers to the middle column of the forefoot during the toe-off phase of stepping, and the forefoot supinates. The lateral column acts during the final phase of push-off while stepping, providing primarily sensory input. The base of the fifth metatarsal alone absorbs significant force and weight. The combination of a fixed midfoot, a slightly flexible Lisfranc joint, and flexible metatarsophalangeal joints create a lever for propulsion during gait.

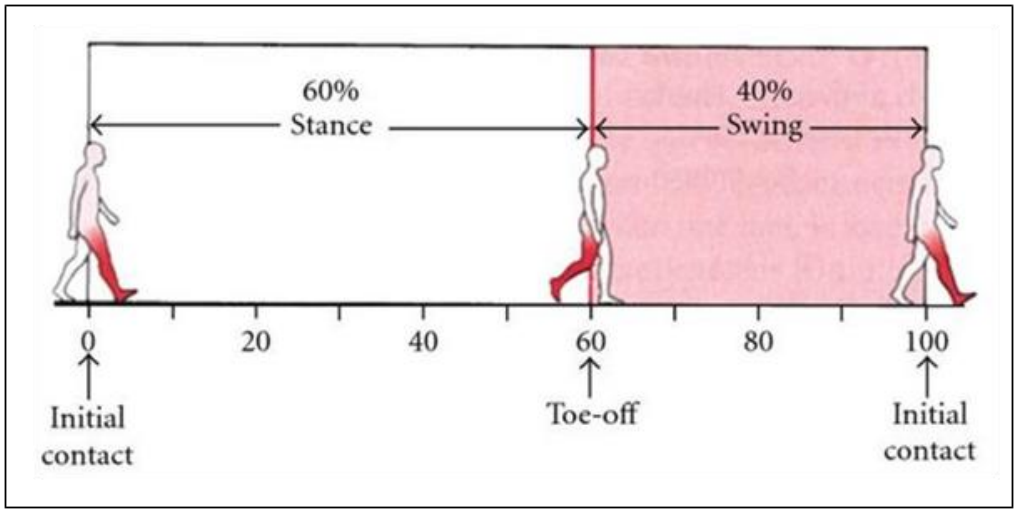


***Figure 3.*** *Human gait.*

### *Range of Motion (ROM) of human foot*

The ankle and foot play a crucial role in our daily activities, from walking and running to maintaining balance and stability. Having a proper range of motion (ROM) in these joints is essential for several reasons: (1) Functional Mobility: Adequate ROM in the ankle and foot allows for smooth and efficient movement, enabling activities such as walking, climbing stairs, and participating in sports; (2) Injury Mobility: Adequate ROM in the ankle and foot allows for smooth and efficient movement, enabling activities such as walking, climbing stairs, and participating in sports; (3) Balance and Stability: Good ROM contributes to better balance and stability, which is vital for preventing falls, especially in older adults; as well as (4) Rehabilitation and Recovery: For individuals recovering from injuries or surgeries, restoring ROM is a key component of rehabilitation, aiding in the return to normal function and activity levels. Understanding and maintaining proper ROM in the ankle and foot is fundamental for overall health and well-being (*Table 1*): (1) Dorsiflexion: Normal ROM values for adults vary from about 15 to 20 degrees in non-weight-bearing positions. Dorsiflexion ROM is affected by the testing position (knee flexed or extended) and whether the measurement is taken in a weight-bearing or non-weight-bearing position; (2) Plantarflexion: Normal ROM values for adults range from about 45 to 55 degrees. Testing is typically done with the individual sitting and the knee flexed to 90 degrees; and (3) Inversion and Eversion: Inversion involves a combination of supination, adduction, and plantarflexion, with normal ROM values for adults varying from about 30 to 35 degrees. Eversion ROM is consistently less than inversion ROM (Norkin and White, 2016).

***Table 1***. *Normal range of motion for adults in degrees.*

| Category | AAOS | AMA | Ma (20-54 yr) M(SD) | Ma (34-40 yr) M(SD) | Fe (18-59yr) M(SD) | Fe (21-59yr) M(SD) |
|---|---|---|---|---|---|---|
| Motion | 20 | 20 | 12.2(4.1) | 15.3(5.8) | 13(9) | - |
| Dorsiflexion | 50 | 40 | 54.3(5.9) | 39.7(7.5) | 60(13) | - |
| Plantarflexion | 35 | 30 | 36.2(4.2) | 27.7(6.9) | 47(9) | 31.5(8.8) |
| Inversion | 15 | 20 | 19.2(4.9) | 27.7(4.6) | 33(10) | 11.1(7.4) |
| Eversion | 20 | 20 | 12.2(4.1) | 15.3(5.8) | 13(9) | - |

*Note: AMA=American Medical Association; AAOS=American Association of Orthopaedic Surgeons; M=Mean; SD=Standard deviation; Ma=Males; Fe=Females.*

### *Load distribution*

The study by Ohlendorf et al. (2020) provides a comprehensive analysis of foot load distribution across different regions in healthy adults aged 18-65 years. Utilizing a pressure measuring plate, the research involved 416 participants (208 male, 208 female) to establish standard reference values for weight and pressure distribution. (1) Balanced Weight Distribution: The study revealed a nearly even distribution of body weight between the left and right feet (50.07% and 50.12%, respectively). Despite this balance, a greater proportion of the load was observed in the rearfoot compared to the forefoot. Specifically, the rearfoot bore 54.14% of the load on the left and 55.09% on the right, while the forefoot supported 45.49% and 44.26% of the load, respectively. (2) Pressure Distribution: The rearfoot experienced higher maximum pressure than the forefoot, with values of 9.60 N/cm² and 9.51 N/cm² for the left and right rearfoot, compared to 8.23 N/cm² and 8.59 N/cm² for the forefoot. Additionally, the study noted that with advancing age, there was a notable shift in load and maximum pressure from the rearfoot to the forefoot. (3) Impact of BMI: The research also highlighted that an increase in Body Mass Index (BMI) was associated with a shift in body weight towards the rearfoot and a rise in maximum pressure across all foot regions. These findings offer crucial reference values for understanding normal foot load distribution in adults and underscore the impact of age and BMI on pressure distribution. Such insights are valuable for clinical assessments and can inform future research into foot biomechanics.

### *Limitations of conventional rehabilitation techniques*

*Subjective Progress Reports*: Traditional rehabilitation often relies on subjective self-reports from patients. These reports can be influenced by various factors, such as patient mood, memory, and perception. Consequently, accurate assessment of progress becomes challenging. *Lack of Objective Monitoring*: Conventional methods lack continuous, objective monitoring. Without real-time data, therapists may miss critical changes or fail to adjust treatment promptly. Objective monitoring tools (e.g., wearable sensors) are underutilized in traditional rehab. *Inconsistent Treatment*: Traditional rehabilitation lacks standardized treatment. As the treatment is highly depedant on skill and knowledge of therpasit and therapists may vary exercise intensity, duration, and frequency based on individual judgment. This inconsistency affects treatment outcomes and hinders evidence-based practice. *Limited Accessibility and Frequency*: Patients often attend in-person sessions at clinics or hospitals. This restricts accessibility, especially for those in remote areas or with mobility issues. Additionally, limited session frequency may slow progress. *Dependency on Therapist Availability*: Patients must align their schedules with therapist availability. Missed sessions due to scheduling conflicts can disrupt continuity of care and hinder recovery. *Cost and Time Constraints*:

Traditional rehab can be expensive due to clinic fees, transportation, and time spent traveling. Moreover, lengthy sessions may not be feasible for patients with busy lives.

### *Cyber-Physical Systems (CPS) in rehabilitation*

The integration of CPS into the realm of rehabilitation has ushered in a transformative era, offering innovative solutions to address the growing demand for effective and accessible therapeutic interventions (Zhang, 2015; Li et al., 2014). As the global burden of chronic conditions and disabilities continues to rise, traditional rehabilitation methods are increasingly challenged to meet the diverse needs of patients (Mawson et al., 2016; Metsis et al., 2013). Enter CPS-a fusion of computational and physical capabilities that harnesses the power of advanced algorithms, sensor technologies, and human- machine interactions to optimize the rehabilitation process (Feng et al., 2021; Zhang, 2015). Conditions such as rheumatoid arthritis (RA) and stroke exemplify the pressing need for innovative approaches to rehabilitation (Mawson et al., 2016; Metsis et al., 2013). Rheumatoid Arthritis (RA), a debilitating disease characterized by joint inflammation and tissue damage, significantly impacts quality of life and increases cardiovascular risks (Metsis et al., 2013. Meanwhile, stroke stands as a leading cause of adult disability, leaving survivors grappling with physical, psychological, and functional limitations (Mawson et al., 2016). Traditional face-to-face rehabilitation services are often constrained by financial and resource limitations, hindering their ability to meet the growing demand (Mawson et al., 2016). CPS-enabled rehabilitation systems offer a compelling solution, leveraging technologies such as vision-based motion tracking, gamification, and intelligent shoe technology to enhance patient engagement, motivation, and adherence (Mawson et al., 2016; Metsis et al., 2013). By integrating personalized feedback, goal-setting, and adaptive treatment protocols, these systems empower individuals to take an active role in their recovery journey, fostering a sense of autonomy and self-efficacy (Mawson et al., 2016; Metsis et al., 2013). Furthermore, the application of CPS in robotics-assisted stroke rehabilitation holds significant promise for improving upper limb movement rehabilitation outcomes (Li et al., 2014). By fostering patient motivation and engagement through gamification and context-sensitive stimulation, CPS has the potential to enhance the effectiveness of such interventions, addressing the limitations of current approaches (Li et al., 2014). The development of CPS-enabled rehabilitation frameworks represents a paradigm shift towards evidence-based patient care (Feng et al., 2021). By harnessing advancements in sensing, data analytics, and machine learning, these systems quantify recovery progress, accumulate knowledge from diverse patient conditions, and enable personalized treatment strategies (Feng et al., 2021). This data-driven approach not only optimizes machine parameters and patient adherence but also offers insights into human-machine interactions and their impact on recovery (Feng et al., 2021). As healthcare systems grapple with the challenges of providing adequate rehabilitation services, the adoption of CPS holds the key to revolutionizing the rehabilitation landscape (Feng et al., 2021; Mawson et al., 2016; Zhang, 2015). By offering accessible, engaging, and personalized interventions, these systems have the potential to foster functional independence, improve quality of life, and ultimately set a new standard for patient care in the digital age (Mawson et al., 2016; Zheng, 2015; Li et al., 2014; Metsis et al., 2013).

### *National Institute of Standards and Technology (NIST) framework for CPS*

A comprehensive framework that aims to establish a structured approach to understanding and developing CPS architectures across various domains, including rehabilitation, is the NIST Special Publication 1500-201 Framework for Cyber-Physical Systems: Volume 1 (Chinn and Hertel, 2010). This framework introduces key concepts such as domains, facets, aspects, and concerns, which collectively form a taxonomy for analysing CPS. The framework emphasizes the unique dimensions of CPS, addressing the interconnectedness and integration of physical and computational components. The NIST framework for CPS serves as a meta-model for deriving domain-specific CPS architectures, ensuring interoperability and facilitating the design, verification, and evolution of complex CPS systems (*Figure 4*). This foundational work aims to establish a common language and methodology for CPS stakeholders, supporting the creation of interoperable and scalable CPS solutions across various applications, including exoskeleton systems for gait assistance and rehabilitation. Based on this framework, a tailored framework is constructed that caters to the deliverables and acts as a pathway to know which features and properties need to be included in the system to make CPS (*Figure 5*).

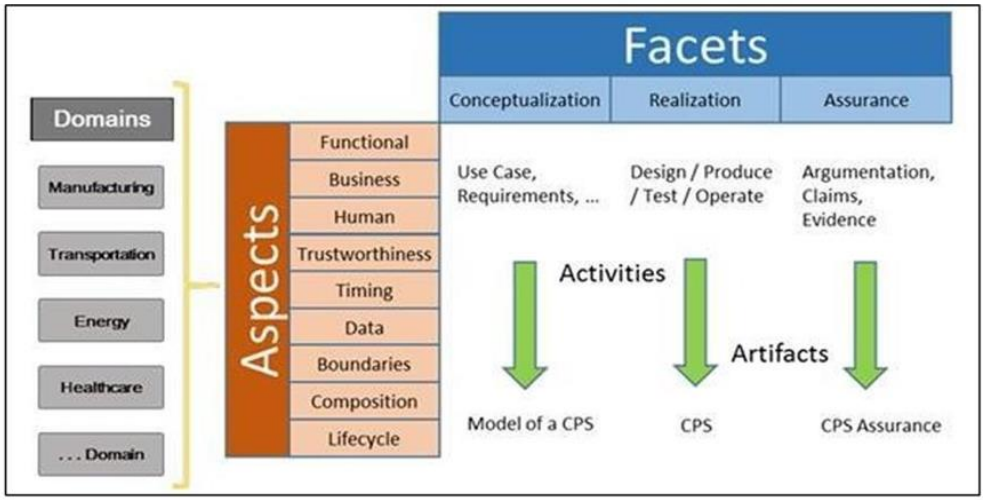


***Figure 4.*** *NIST framework for CPS.*

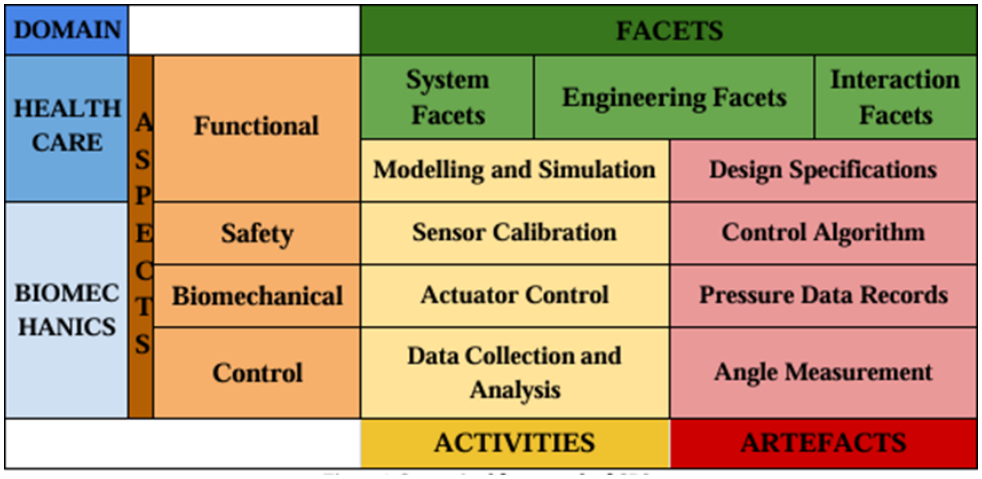


***Figure 5.*** *Adapted NIST.*

## Materials and Methods

### *Design and development of a mechatronic Cyber-Physical medical device components*

The device designed for monitoring and aiding in the rehabilitation of lower extremities consists of two primary components: the wearable part and the control unit carrier. (1) The wearable part is constructed from lightweight aluminium, ensuring that the device is durable yet comfortable enough to be worn directly on the skin. This component is secured to the calf using Velcro straps, which provide a snug fit and prevent slipping during walking activities. Embedded within the insole of this wearable part are Force-Sensitive Resistors (FSRs) that continuously measure the plantar pressure distribution across the patient's foot. This capability is crucial for assessing the load and weight distribution during different phases of gait (*Figure 6*). (2) The control unit carrier houses the microcontrollers, electronic systems and power source necessary for the device's operation. This includes two Arduino microcontrollers Arduino MEGA and Arduino UNO to process the FSR data and MPU-6050 data respectively. Two DC motors and Bowden cables, which are responsible for providing the mechanical assistance required to pull the heel and facilitate walking. The control unit also integrates two MD-10 motor drivers to control the actuation direction of the motors. By focusing on this single degree of freedom (DOF), the device simplifies the rehabilitation process, concentrating on the essential movements needed for effective rehabilitation (*Figure 7*).

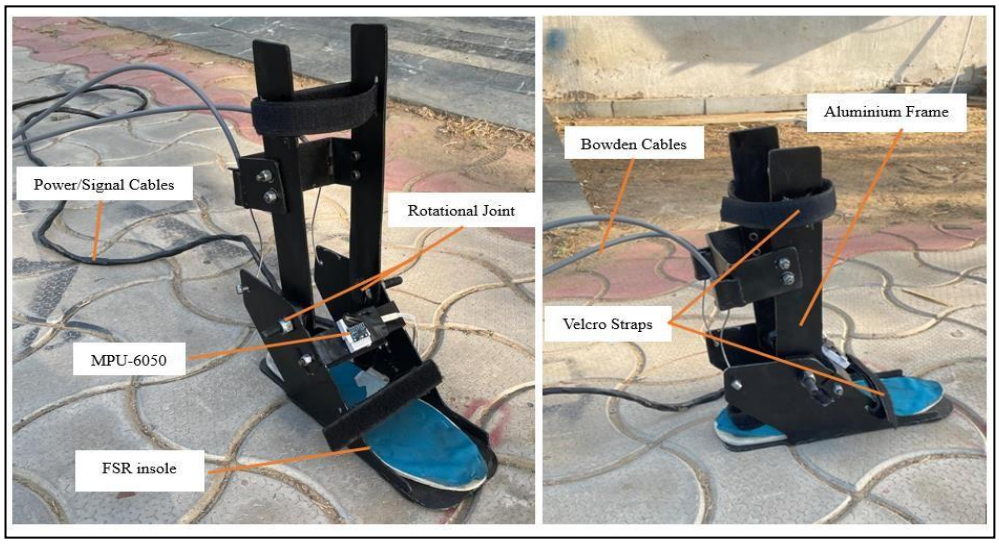


***Figure 6.*** *CPS based ankle rehabilitation device (wearable part).*

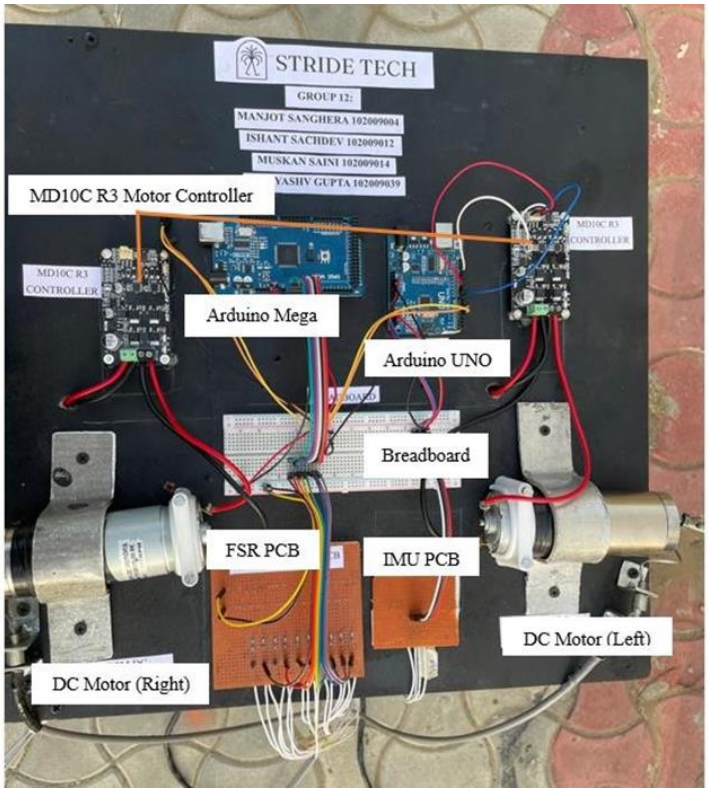


***Figure 7.*** *CPS based ankle rehabilitation device (control unit carrier).*

### *System components and connections*

The system comprises several key components (*Figure 8*):

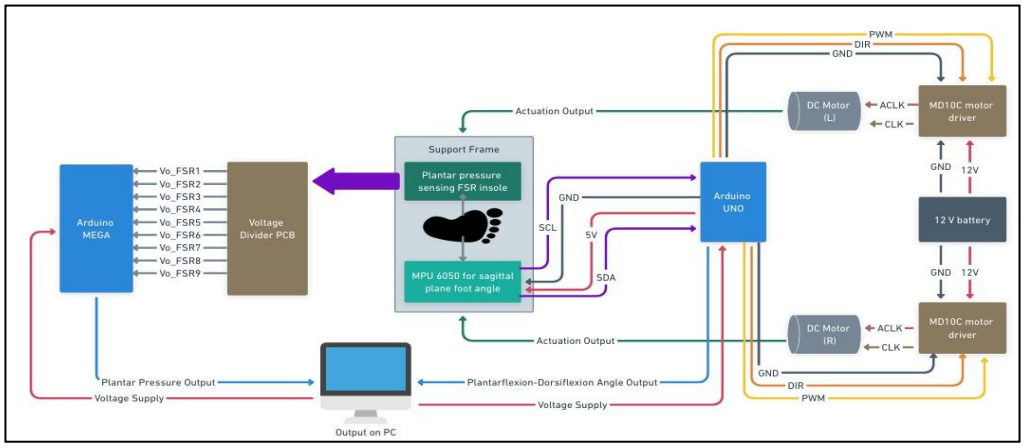


***Figure 8.*** *Functional flow of rehabilitation device.*

*Arduino Mega and Arduino UNO*: The Arduino Mega and Arduino UNO are microcontroller boards used for processing and controlling the system's operations. The Arduino Mega handles the input from the plantar pressure sensors and sends this data to the PC for analysis. The Arduino UNO controls the DC motors based on the input from the MPU 6050 sensor and the plantar pressure data.

*Voltage Divider PCB*: The Voltage Divider PCB is used to convert the analog signals from the force-sensitive resistors (FSRs) in the insole to a voltage level that the Arduino

Mega can read. This ensures accurate measurement and processing of the plantar pressure data.

*Plantar Pressure Sensing FSR Insole*: The FSR insole measures the plantar pressure distribution across different areas of the foot. This data is crucial for assessing the patient's gait and detecting areas of high pressure, which can help in tailoring the rehabilitation process.

*MPU 6050 Sensor for Sagittal Plane Foot Angle*: The MPU 6050 sensor is an inertial measurement unit (IMU) that tracks the dorsiflexion and plantarflexion angles of the ankle in the sagittal plane. This data is used to monitor the range of motion and assist in the rehabilitation exercises by controlling the DC motors to provide the necessary support.

*Arduino UNO*: The Arduino UNO controls the actuation of the DC motors based on the data received from the MPU 6050 sensor and the FSR insole. It ensures the motors provide the correct amount of assistance during rehabilitation exercises.

*DC Motors and Motor Drivers*: The DC motors, controlled by motor drivers, are used to assist the patient's movement by pulling the heel through Bowden cables. They provide the necessary force to aid in dorsiflexion and plantarflexion during rehabilitation exercises.

*12V Battery*: The 12V battery supplies power to the DC motors and the motor drivers. It ensures that the motors have enough power to provide the required assistance during the rehabilitation process.

*PC Interface*: The PC interface is used to display the plantar pressure and foot angle data in real-time. It allows physiotherapists to monitor the patient's progress, adjust the rehabilitation parameters, and analyze the effectiveness of the treatment.

### *Plantar pressure measurement*

The Plantar Pressure Sensing FSR Insole embedded in the support frame is equipped with multiple Force-Sensitive Resistors (FSRs) that measure plantar pressure at various points across the sole of the foot. These sensors detect the distribution of pressure when the patient stands, walks, or performs rehabilitation exercises.The FSRs generate voltage outputs corresponding to the pressure applied. These outputs are then routed to the Voltage Divider PCB, which conditions the signals to be readable by the Arduino Mega. The Arduino Mega processes these signals, translating them into plantar pressure data. This data is subsequently outputted to a connected PC for visualization and further analysis. The real-time plantar pressure data allows clinicians to assess the patient's weight distribution and identify any abnormalities.

### *Ankle movement measurement*

The device uses an MPU 6050 sensor mounted in the support frame to measure the dorsiflexion and plantarflexion angles of the ankle. This Inertial Measurement Unit (IMU) provides precise measurements of the ankle's movements in the sagittal plane. The IMU communicates with the Arduino Uno via the I2C protocol, using the SDA (Serial Data) and SCL (Serial Clock) lines. The Arduino Uno processes the angle data and sends it to the PC, where it can be monitored and recorded. This data helps in assessing the range of motion and flexibility of the ankle, providing valuable insights for rehabilitation progress.

### *Mechanical assistance*

To assist patients during rehabilitation, the device incorporates a mechanical system comprising DC motors and Bowden cables. The Arduino Uno controls these motors, which are powered by a 12V battery. Each motor is connected to an MD10C motor driver that regulates the motor's speed and direction. The motor drivers receive Pulse Width Modulation (PWM) signals from the Arduino Uno to control the actuation of the motors. Additionally, directional (DIR) signals are provided to ensure proper movement. The DC motors are responsible for pulling the heel through the Bowden cables, thereby assisting the patient in achieving the desired dorsiflexion and plantarflexion movements. The actuation thresholds can be set based on the patient's effort, allowing for customizable assistance tailored to the individual's progress.

### *System integration and user interface*

The integration of the plantar pressure measurement, ankle movement tracking, and mechanical assistance systems is facilitated through the central control provided by the Arduino Mega and Arduino Uno. The entire system is powered by the 12V battery, ensuring that the device is portable and can be used in various settings. The data from the plantar pressure sensors and the IMU is continuously transmitted to a PC interface, where clinicians can monitor and adjust the device's settings. The PC interface allows for the visualization of real-time data, making it easier for clinicians to track the patient's progress and make necessary adjustments to the rehabilitation program. The customization of motor actuation thresholds is also managed through this interface, ensuring that the assistance provided is optimal for the patient's current rehabilitation stage.

### *Evaluation of parameters for detailed design and analysis*

To ensure the proper analysis before fabrication of the product following parameters were evaluated to ensure that the device works properly.

### *Foot pressure estimation for Finite Element Analysis (FEA)*

As such there exists no metric for evaluating the foot surface area, and these measurements are either evaluated from indirect calculation or by manual measurement by using methods like ink dipping. For our case we decided to use the indirect calculation approach by using the medical tools like:

*Body Surface Area*: This is one of the most significant indices of physiological functions in pediatric practice and child health is total body surface area (TBSA). The determination of BSA is a necessary step in making accurate assessment of some organ functions and for making decision on many critical treatments' plans (Orimadegun and Omisanjo, 2014). To evaluate total a mathematical equation was derived by DuBois and Du Bois (1916), which is as follows (Eq. (1):

$$TBSA[m^2] = Weight[kg]^{0.425} \times Height[cm]^{0.725} \times 0.007184 \qquad \text{Eq. (1)}$$

*Lund Browder Chart*: The Lund and Browder (LB) chart is currently the most accurate and widely used chart to calculate total body surface area affected by a burn

injury. Referring to this chart we are able to evaluate what percentage of the TBSA is composed of foot surface area (FSA), thus giving us our required area (*Figure 9*).

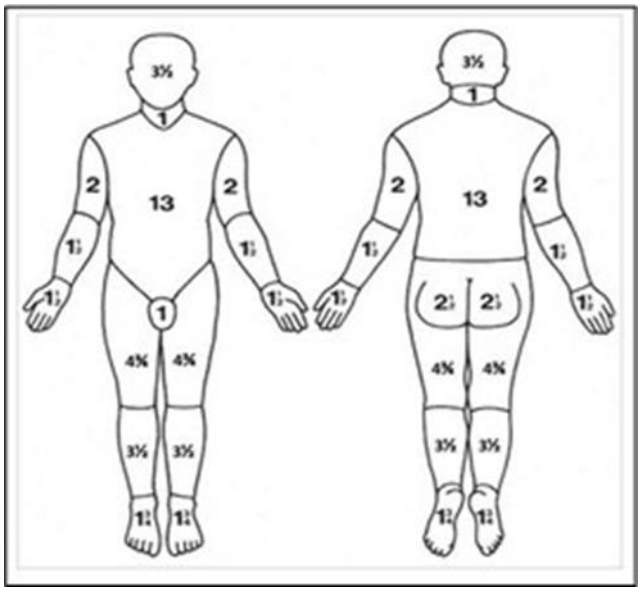


***Figure 9.*** *Lund Browder chart.*

Based on the metric requirements obtain the sufficient and necessary data: From the identified metrics, we need to know the Age, Body weight in kilograms, height in centimetres and shoe size (UK) to decide the dimensions and load for analysis. To do this a google form was circulated. Evaluation of the foot surface area according to metrics: Following equations were used to calculate FSA as (Eq. (2):

$$FSA[m^2] = 0.0175 \times TBSA$$
$$Force\ [N] = Mass \times acceleration\ due\ to\ gravity\ (9.81\ m/s^2)$$
$$\text{Pressure [KPa]} = \frac{Force\ [N]}{FSA\ [m2]} \qquad \text{Eq. (2)}$$

### *Evaluation of the torque of the motors*

*Torque estimation*: The Achilles tendon supports the entire weight when a person is doing activities like jumping, walking, stepping, therefore it is necessary to know the force of the tendon, which then can be used to determine the torque. For the evaluation of this force certain assumptions are made, consider a foot at an angle of 15° inclined from ground, the length from toes to point where Achilles tendon is attached is 25cm, the assumption about foot length is made using the data from the survey therefore the distance from where the bone attaches to the pivot point at the back of the foot to the toes is 18cm. The weight of a person is assumed to be 80 kgs ~800N. Based on this assumption a Free Body Diagram FBD shown in *Figure 10* is constructed.

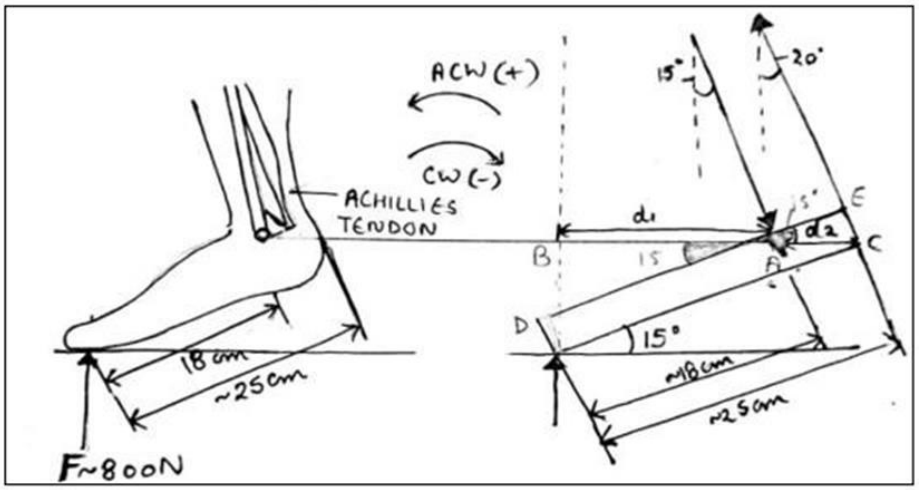


***Figure 10.*** *Free body diagram of foot with reaction forces.*

Force F is perpendicular to the distance from the line of action of the force to the pivot point A which d1, and the FA acts at a distance of d2 from the pivot point. So, the summation of all forces is (Eq. (5):

$$\Sigma T_A = -(800).d1 + FAd2 = 0 \qquad \text{Eq. (3)}$$

To find the distance d1,it is known that the distance from the point of ground reaction to the pivot is 18cm inclined at an angle of 15°. Also, BA is parallel to ground, so the angle BAD is also equal to 15°. Length d1 being adjacent to BAD results in the value of length as 18cos(15°). So equation-1 becomes (Eq. (4):

$$\Sigma T_A = -(800).18cos\,(15°) + FAd2 = 0 \qquad \text{Eq. (4)}$$

To determine the distance d2, we know that length AC=25-18=7 cm. And FA is acting at an angle of 20°, thus considering the *Figure 11* where force is attached to the beam at an angle Φ relative to vertical. So, if the foot is at an angle 15°, and 20° relative to the vertical, the angle Φ comes out to be Φ20-15=5°. Therefore d2=7.cos(5°)-put in Eq. (5).

$$\begin{aligned} \Sigma T_A &= -(800).18cos\,(15°) + FA.7\,cos\,(5°) = 0 \\ &\Rightarrow (800).18cos\,(15°) = FA.7\,cos\,(5°) \\ &\therefore FA = \frac{(800).18\cos\,(15°)}{7\cos(5°)} = 1995\,N\ or\ 1.995\,kN \end{aligned} \qquad \text{Eq. (5)}$$

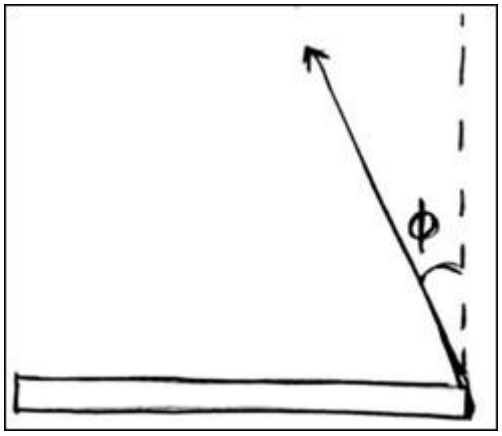


***Figure 11.*** *FBD for evaluating angle of force of Achillies tendon.*

An Achilles tendon length below 6 cm is strongly related to a higher ankle range of dorsiflexion (Góes et al., 2015) so taking the value of moment arm length for the Achilles tendon and ankle to be 5 cm or 1.05 m, the torque required for a healthy body's ankle to take and maintain and plantarflexion of 15° is: $r=FA$×0.05=1995×0.05=99.75$Nm$ For the system of assistance, the level of assistance is minimal meaning the patient will perform 75% of work and the device will perform 25% of the work (Kim et al., 2019). Therefore, the required torque is, Tperson=0.75×Ttotal; $T$motors=0.25×$T$total. Given that the total torque $T$total is 99.75 Nm (calculated earlier), we can now compute the contributions: (1) Person's Contribution [$T$person=0.75×99.75Nm=74.8125Nm]; (2) Device's Contribution [$T$motors=0.25×99.75Nm=$T$motors=24.9375Nm]. Thus, the minimal torque of 24.9375 Nm is required by our system. *Angular Velocity Calculation*: With a swing phase duration of 3 seconds:

$$\omega = \frac{Motor\ Torque}{t} = \frac{24.9375Nm}{3} = 8.3125rad$$

Power Calculation: P=T·ω=24.9375 Nm·8.3125 rad/s=207.34 W
RPM Calculation:

$$RPM = \frac{P}{T} X \frac{60}{2\pi} = \frac{207.94}{24.9375} X \frac{60}{2\pi} = 79.4RPM$$

With the weight of 80 kg, a swing phase duration of 3 seconds, and the motor providing only 25% of the lifting torque, the motor needs to operate at approximately 79.4 RPM to lift the foot with the torque requirement of 24.9375 Nm.

### *CAD modelling and FEA analysis*

*Wearable part*: This member acts a foot rest, that will be worn by the user on their foot, this component provides the support and controlled motion to user's foot (*Figure 12*). *Control Unit Carrier*: this is the heart of the system, all the microcontrollers, motor drivers and motors are embedded on this carrier and the sensors are connected to the microcontroller by wires and the foot rest is connected to motors by Bowden cables (*Figure 13*).

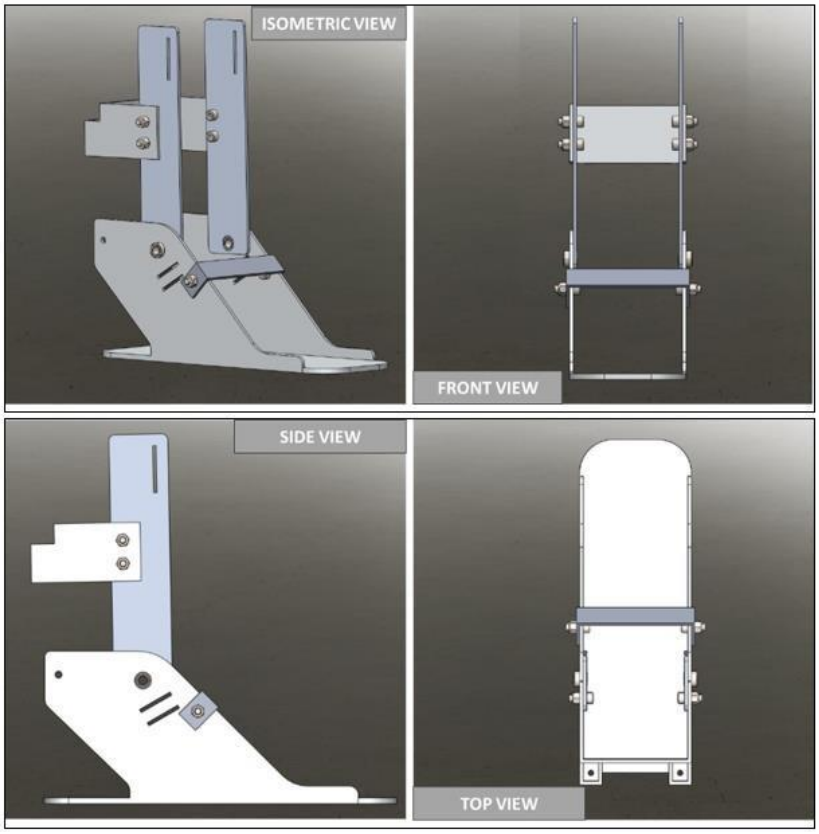


***Figure 12.*** *Isometric, Front, Side and Top views of wearable part.*

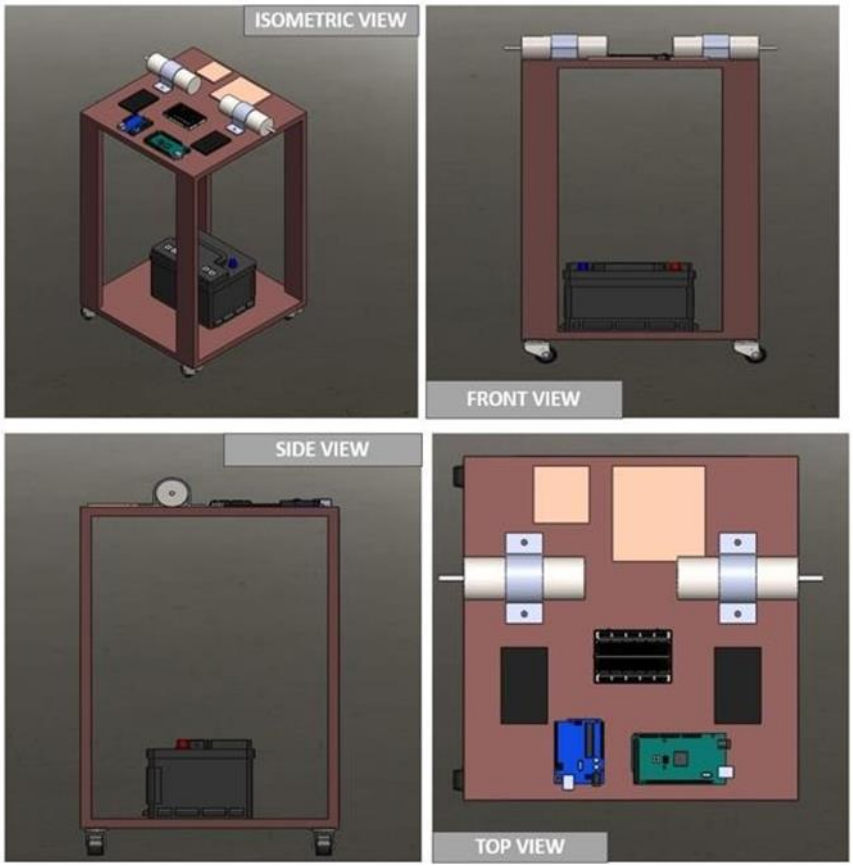

***Figure 13.*** *Isometric, Front, Side and Top views of Control Unit Carrier.*

### *Finite Element Analysis (FEA)*

### *Total deformation (Boundary conditions)*

*Calf Supports Constrained*: All six degrees of freedom (DOF) of the calf supports were constrained. This means that the calf supports were fixed in place and not allowed to translate or rotate in any direction. This simulates the condition where the calf supports are firmly attached to a stable structure, ensuring no movement during the analysis. *Simulated Foot Movement Forces*: To simulate the movement of the foot, an upward force of 5.6N was applied at one end of the foot rest, while an equal downward force of 5.6N was applied in the opposite direction at the other end. These forces mimic the dynamic action of the foot moving up and down, creating a bending effect on the foot rest. *Self-Weight Force*: The base foot was subjected to a force corresponding to the self- weight of the person using the device. This force was applied to represent the static load due to the weight of the user, ensuring that the analysis accounts for the overall stress and strain the device would experience under normal conditions (*Figure 14*).

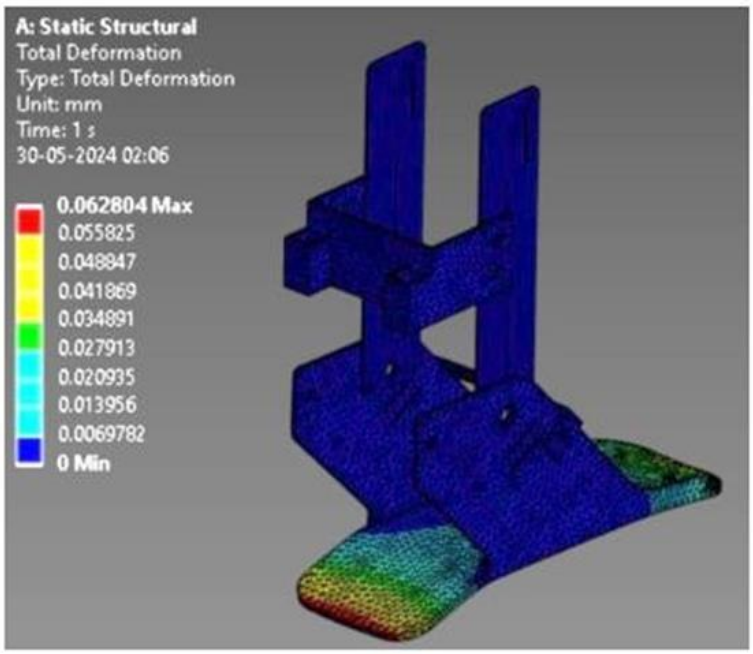


***Figure 14.*** *Total deformation analysis of wearable part.*

The deformation analysis image provides a color-coded representation of the total deformation experienced by the foot rest under the applied boundary conditions. The deformation is measured in millimetres, with the colour scale indicating the extent of deformation at various points on the structure. Here are the key observations from the results: (1) *Maximum Deformation*: The highest deformation recorded is approximately 0.00012816 mm. This value is extremely small, indicating that the foot rest structure is highly rigid and capable of withstanding the applied forces without significant bending or deformation; (2) *Deformation Distribution*: The majority of the structure shows minimal deformation, as indicated by the blue and green regions. This suggests that these areas are under low stress and remain relatively stable.The areas with higher

deformation, transitioning into yellow and red, are localized and do not compromise the overall integrity of the foot rest. These regions are likely where the applied forces have the most direct impact; and (3) *Structural Integrity*: The small values of deformation across the structure demonstrate that the foot rest is well- designed to handle the applied loads. The constrained calf supports effectively immobilize the structure, while the forces simulating foot movement and self-weight are within the material's capacity to endure without causing failure or significant deformation.

***Von-mises stress (Boundary conditions)***

*Calf Supports Constrained in All 6 Degrees of Freedom (DOF)*: The calf supports are completely fixed, meaning they cannot move or rotate in any direction. This implies constraints in all three translational (X, Y, Z) and all three rotational (about X, Y, Z axes) degrees of freedom. This setup ensures that the calf supports act as a rigid support, providing stability and replicating the real-life scenario where the calf support is firmly attached and doesn't move. *Upward and Downward Forces to Simulate Foot Movement*: A force of 5.6 N is applied upwards on one end of the footrest along with a force of 5.6 N is applied downwards on the opposite end. These forces simulate the dynamic action of a foot moving on the footrest, creating a moment and potentially causing bending and shear stresses in the structure. *Self-Weight of the Person Applied to the Base Foot*: The weight of the person sitting on the footrest is considered as a force acting on the base of the footrest. This force is distributed according to the weight of the person, creating compressive stress in the structure. The exact value of this force is not specified but would typically be the weight of an average person (e.g., 70-100 kg) (*Figure 15*).

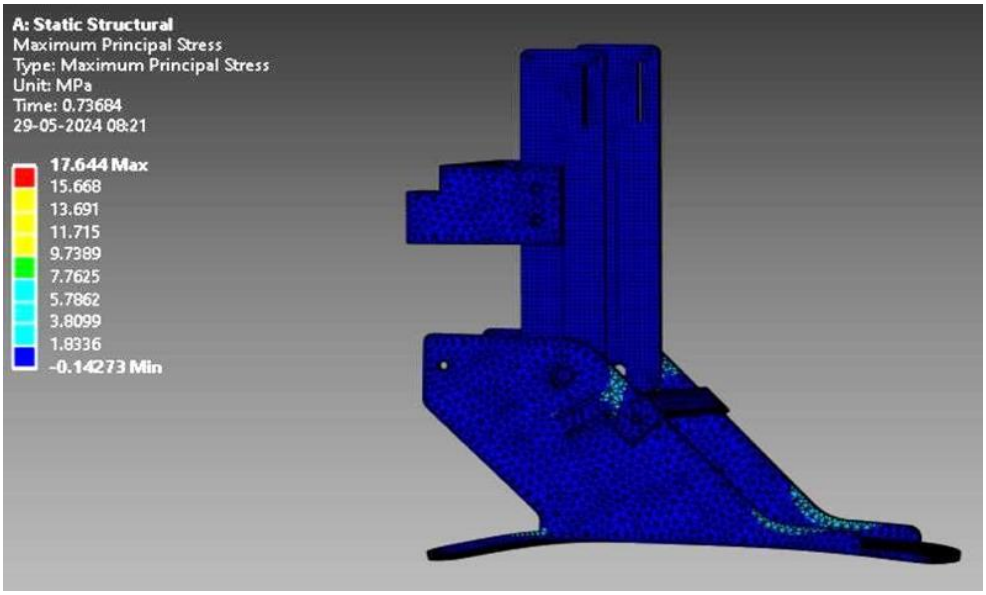


***Figure 15.*** *Von Misses analysis of wearable part.*

*Maximum Principal Stress*: The analysis indicates a maximum principal stress of 17.644 MPa in the structure. The stress distribution is visualized in the provided image, with areas of higher stress highlighted in red and lower stress areas in blue and green. The maximum stress is concentrated in regions experiencing the greatest deformation due to the applied forces, likely around the points of applied force and constrained supports. *Factor of Safety (FOS)*: The Factor of Safety is calculated as the ratio of the

material's yield strength to the maximum principal stress observed. Given: Material's yield strength=310 MPa, Maximum observed stress=17.644 MPa FOS=310/17.644=17.57 This high FOS indicates that the footrest structure is significantly over- designed for the given loading conditions, suggesting a robust design capable of withstanding much higher loads than those applied in this simulation. *FSR calibration*: To use the FSR with Arduino, the sensor is connected in a voltage divider circuit as shown in the figure19 (left) and this arrangement makes the FSR as a variable resistance or a rheostat whose resistance can be varied by applying force. To know the output voltage from the voltage divider following equation is used (Eq. (6):

$$V_{out} = R_0 X \frac{V_{cc}}{(R_0 + R_{fsr})} \qquad \text{Eq. (6)}$$

The calibration setup shown in the Figure16 (right), the force acting on the FSR was gradually increased by using the scale weights and the readings of the resistance were taken by implementing the Arduino. Following plot between the load and output voltage was obtained to know the linearity characteristic between the input load and output. figure is the characteristic curve obtained (*Figure 17*).

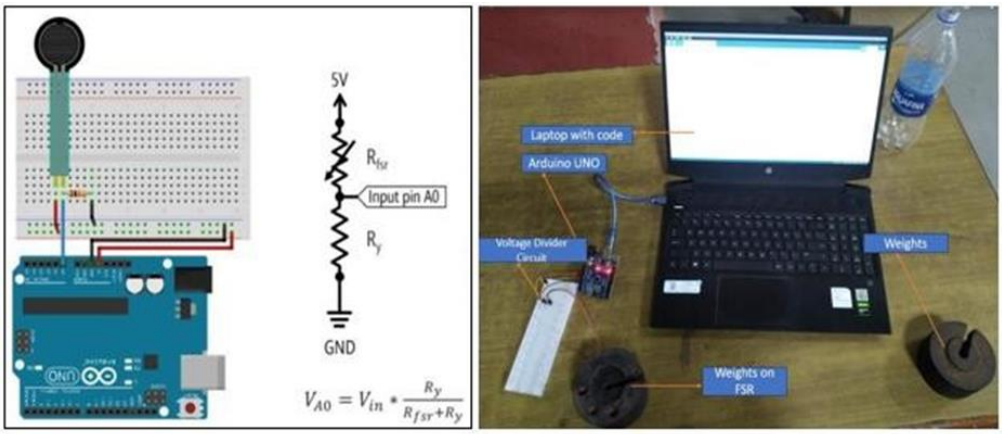


***Figure 16.*** *FSR connection with Arduino(left). Calibration setup of FSR(right).*

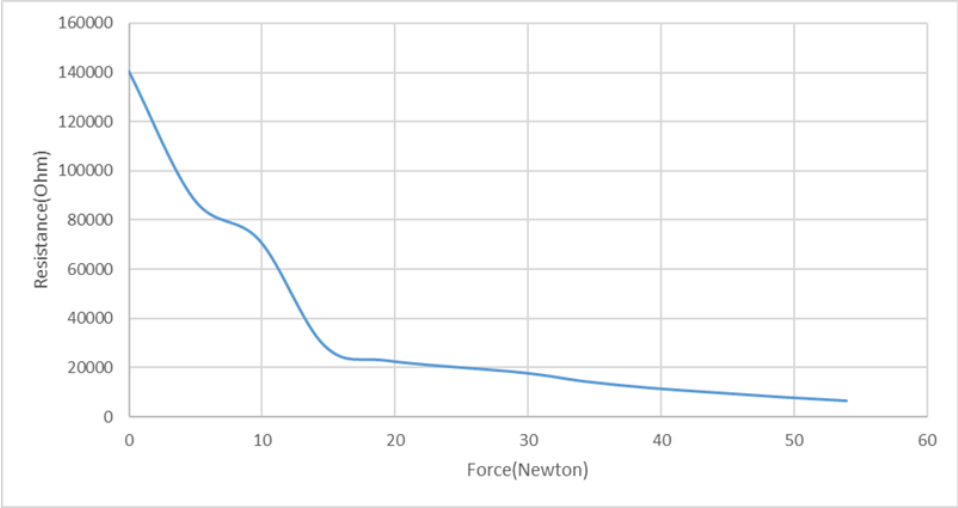


***Figure 17.*** *Output of FSR calibration.*

*FSR Instrumentation*: To implement the pressure sensing functionality of the device, the FSRs were embedded on a sole, following a chart about the key pressure points was referenced to know the positions of the FSRs so that essential information about the pressure points is obtained. The number of the FSRs is dependent on the available area and the size of the FSR's active area therefore the quantity of FSR can be changed as required whereas the positions need to be exact (*Figure 18*). Following *Figure 19* block diagram explains the code logic used to evaluate the pressure in the forefoot, midfoot and hindfoot.

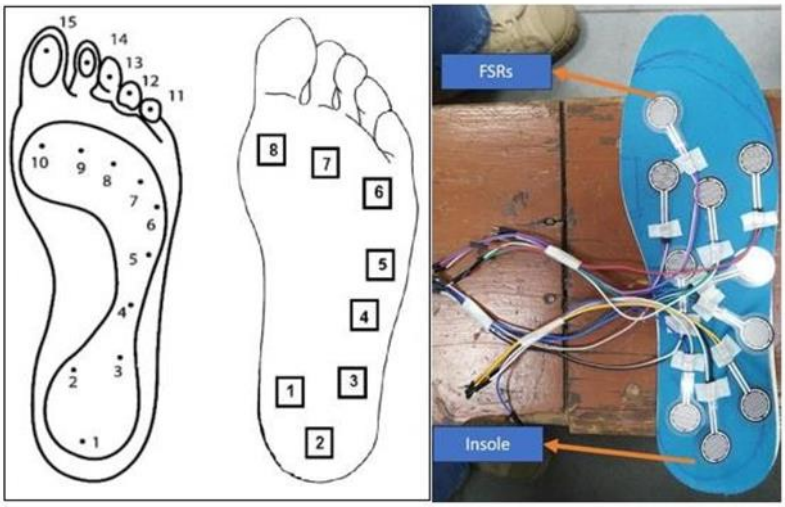


***Figure 18.*** *Pressure points of Human foot (left). FSR positioning on insole (right).*

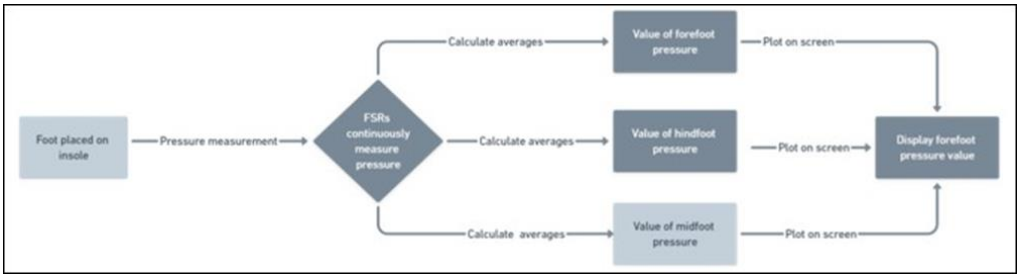


***Figure 19.*** *Functional flowchart for FSR instrumentation.*

MPU Instrumentation and Calibration: Following *Figure 20* block diagram explains the code logic used to evaluate the pressure in the forefoot, midfoot and hindfoot. To calibrate the MPU, an experimental setup was constructed as shown in figure, MPU was mounted onto a shoe and following steps were followed to calibrate the MPU so that mounted position is considered as zero position, this experiment resulted in the calibration parameters for mounting positions and a plot depicting the plantarflexion and dorsiflexion of foot while walking (*Figure 21*). (1) After mounting, keep the shoe parallel to ground, observe the value of acceleration in the Z axis, it should be one, if not add or subtract the required factor to make the observed value equal to one. (2) Turn the shoe so that the pitch angle reaches value of one, if the observed acceleration in the Y axis is not equal to one, add or subtract the required factor to make the observed value one. (3) Similarly turn the shoe so that acceleration in X direction is one and add or subtract the required factor to make the observed value one.

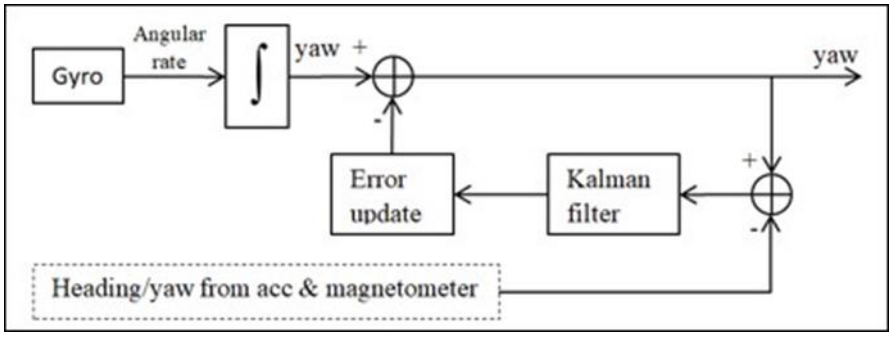


***Figure 20.*** *Functional flowchart of Kalman filter.*

***Figure 21.*** *Instrumentation of MPU6050.*

### *Motor integration*

The DC motors are chosen for their ability to deliver consistent torque and precise movement control, which are essential for mimicking natural walking patterns. By integrating these motors into our system, we can provide dynamic assistance to the user, adjusting in real-time to their walking needs and maintaining the desired foot angle. These motors are controlled by MD10C motor driver by Cytron (*Figure 22* angle *Figure 23*). Which is specifically designed to handle the power requirements and provide the necessary precision in motor control. It interfaces seamlessly with our central microcontroller, the Arduino MEGA, which sends PWM signals to the motor driver based on the data received from sensors monitoring the foot angle and plantar pressure. The process of controlling the motors involves the following steps: (1) *Sensor Data Collection*: The MPU6050 foot angle sensor collects real-time data on the user's walking pattern and foot position; (2) *Data Processing*: The Arduino MEGA processes this sensor data to determine the current plantarflexion angle and the required adjustments to assist movement; (3) *Signal Generation*: Based on the processed data, the Arduino MEGA generates PWM control signals that are sent to the MD10C motor driver; (4) *Motor Actuation*: The MD10C motor driver interprets these signals and adjusts the power supplied to the DC motors, ensuring they operate within the specified

range of motion (+20 to -20 degrees); and (5) *Feedback Loop*: Continuous feedback from the sensors allows for real-time adjustments, maintaining optimal motor performance and ensuring the foot remains within the desired angle range.

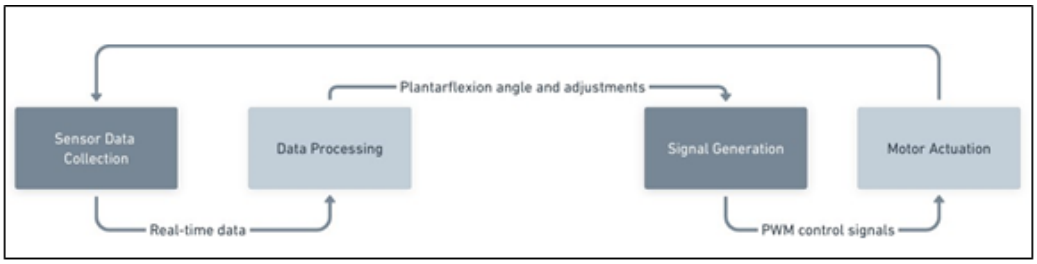


***Figure 22.*** *Functional flowchart of motor control.*

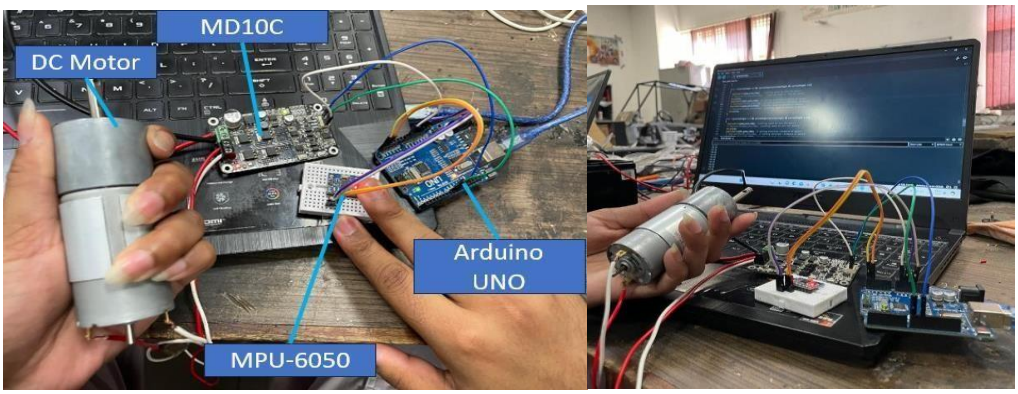


***Figure 23.*** *Motor testing with MPU-6050.*

### *Testing of motion of foot*

The Figure 24 showing the assisted walk stances while wearing the foot rest. These photographs depict a person wearing the wearable subpart of the device on their right foot: (1) The device has a rigid structure that extends from the ankle to the toes, to provide support and potentially allowing for the measurement or restriction of certain foot movements; (2) In the first photograph, the person is standing with their feet slightly apart, representing the initial stance or starting position for a walking trial; (3) From the rest position the person takes the first step with their free foot and proceed to walk with the device as seen in second photograph, the weight of the person, and one foot is slightly lifted off the ground, beginning of the swing phase of the gait cycle with the assistance from the Bowden cables and motors; and (4) In the third photograph, the person's foot is under the process to make the heel contact with the floor and complete the step. This process repeated over the course of exercise duration allowing the patient to move the foot in the correct range of plantarflexion and dorsiflexion.

***Figure 24.*** *Walk stances while wearing foot rest: rest, swing, stride.*

### *Plantarflexion and Dorsiflexion measurements of the device*

The theoretical plot (*Figure 25*) of plantarflexion and dorsiflexion, which are the downward and upward movements of the foot, respectively. The plot shows the angle of the ankle relative to the percentage of the gait cycle. It has three distinct regions labeled as ROM1, ROM2, and ROM3, representing different ranges of motion (ROM) during the gait cycle (Góes et al., 2015). The theoretical plot Figure-61 shows a smooth, idealized curve, while the actual plot (*Figure 26*) has some noise and irregularities, as expected from real-world measurements. The theoretical plot covers the entire gait cycle (0-100%), while the actual plot only shows data for two steps, which is a smaller portion of the complete gait cycle. The general shape and patterns of the two plots are similar, with the actual plot exhibiting the expected plantarflexion and dorsiflexion movements, but with some variations from the theoretical curve. The theoretical plot provides a reference for the expected range of motion and timing of the ankle movements, while the actual plot shows how these movements occur in practice, with the influence of various factors such as individual gait patterns, measurement errors, and external conditions.

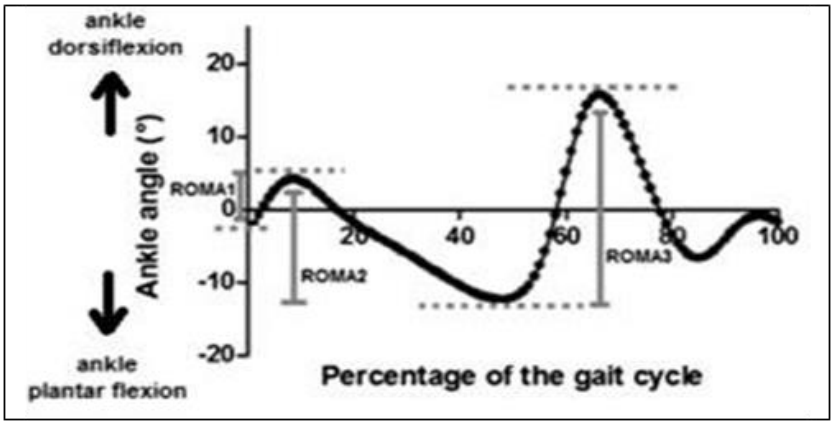


***Figure 25.*** *Theoretical plot of plantarflexion and dorsiflexion.*

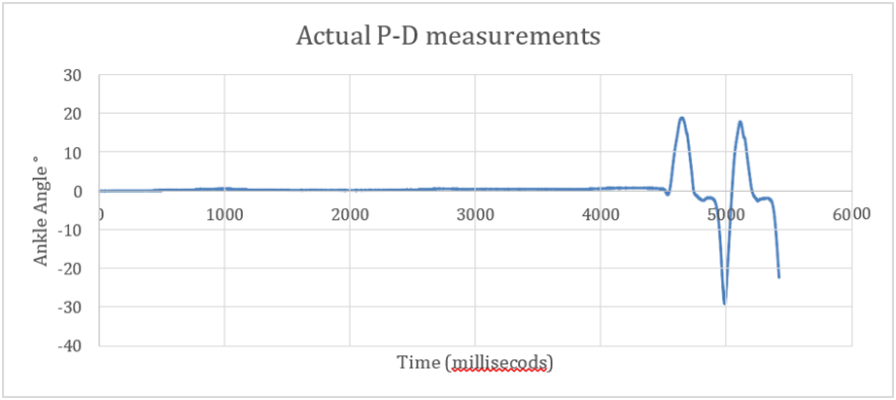


***Figure 26.*** *Actual plantarflexion and dorsiflexion output.*

### *Plantar pressure monitoring using device*

The theoretical plot (*Figure 27*) shows a theoretical plot of plantar pressure, which represents the pressure distribution on the foot during different phases of the gait cycle (walking). The plot displays several curves, each labelled with a number from s1 to s10, representing different sensors or regions on the foot (Kim et al., 2019). The actual plot (*Figure 28*) shows three distinct peaks, corresponding to the heel strike, midfoot contact, and toe-off phases of the gait cycle. The heel and forefoot regions exhibit the highest pressure during these phases, while the midfoot region experiences lower pressure. The theoretical plot (*Figure 27*) provides an idealized representation of plantar pressure distribution, while the actual plot (*Figure 28)* shows the real-world plantarflexion movements of different foot regions. The theoretical plot focuses on pressure values, while the actual plot displays the average pressure put on by the patient in the forefoot, midfoot and hindfoot. The three peaks in the theoretical plot correspond to the different portions of the foot during gait cycle, which can be correlated with the peaks and movements observed in the actual plot. The theoretical plot shows smoother curves, while the actual plot exhibits more irregularities and noise, as expected from real-world measurements. The theoretical plot provides a general reference for the expected pressure patterns, while the actual plot allows for analysis of specific foot regions and their movements during the gait cycle.

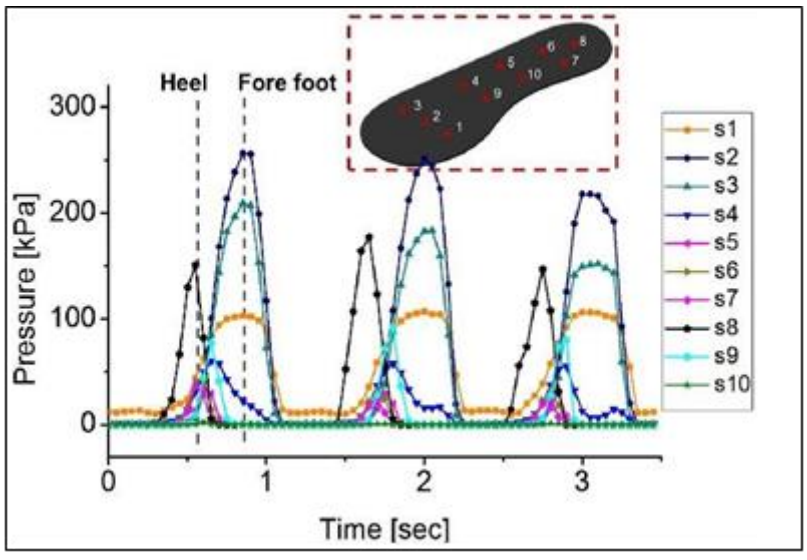

***Figure 27.*** *Theoretical plot of plantar pressure.*

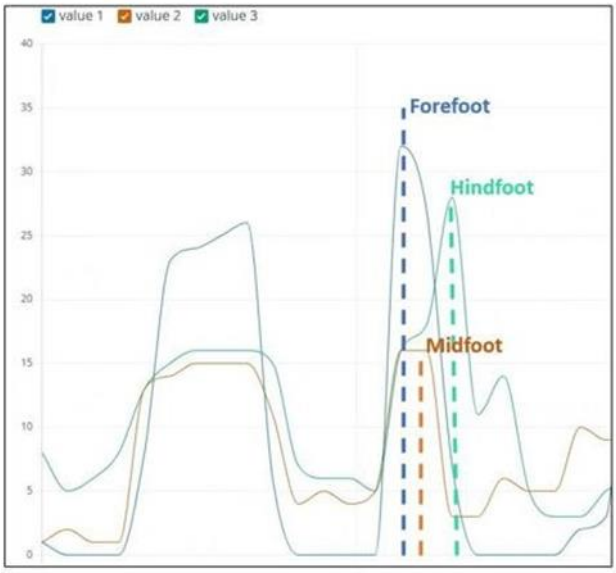


***Figure 28.*** *Actual plantar pressure output.*

The development of the mechatronic cyber-physical medical device for monitoring lower extremity rehabilitation began with a thorough problem identification and ideation phase. Market and literature reviews provided insights into existing technologies and their limitations, guiding the design process. The fabrication phase involved planning and executing the construction of the prototype, which incorporated a force-sensing resistor (FSR) embedded insole for plantar pressure measurement and an IMU-MPU6050 sensor for dorsiflexion and plantarflexion angle measurement. Testing was conducted to validate the basic functionality and performance of the prototype. The initial testing of the prototype demonstrated its ability to measure plantar pressure distribution and dorsiflexion/plantarflexion angles accurately. The FSR insole provided real-time pressure data, while the IMU sensor effectively captured ankle angles. The system's responsiveness, particularly the actuation of motors using Bowden cables to assist in walking, was observed to be between the -20 degrees to +20 degrees with an error of few degrees. However, several technical challenges were noted, such as occasional sensor inaccuracies and the need for more precise motor control.

Several limitations were identified during the development and testing phases. Technical limitations included sensor inaccuracies and motor control issues, which impacted the overall performance of the system. Time constraints also played a significant role, as the project was completed within a year, limiting the scope of testing. Notably, no actual patient testing was conducted, primarily due to time limitations and patient safety concerns. Another significant limitation of the device is its current design, which only allows the patient to take two steps forward due to the length constraint of the Bowden cables. Although the control unit carrier includes wheels to facilitate movement, this restriction limits the practicality of the device for continuous walking exercises. A potential solution for this limitation is the incorporation of a treadmill, which would enable continuous movement and a more comprehensive rehabilitation process. Future work will focus on conducting patient trials to assess the device's efficacy and safety in a clinical setting. Plans for technical improvements include integrating more advanced sensors to enhance measurement accuracy,

improving the robustness of the system, and enhancing data analysis capabilities. Addressing the current limitation of the device's range, integrating a treadmill into the setup will be a priority to allow for continuous walking exercises. Additionally, to improve motor actuation control, incorporating more reliable factors such as myosensors to monitor myosin protein levels in muscles can lead to more effective motor actuation. Furthermore, a specialized foot pressure sensing array would be a significant addition to the project, overcoming the limitation of the sole size and providing more reliable and detailed information about foot pressure distribution. Ensuring patient safety will be a priority in future testing, with thorough risk assessments and adherence to medical device regulations. The potential clinical applications of the device are significant, particularly in aiding physiotherapists in monitoring patient progress and customizing treatment plans. The device could improve patient outcomes by providing real-time data and personalized rehabilitation protocols. Additionally, the broader implications of the device include its potential to reduce healthcare costs and enhance the effectiveness of lower extremity rehabilitation.

## Conclusion

The development of a mechatronic cyber-physical medical device for monitoring lower extremity rehabilitation represents a significant step forward in the field of physiotherapy and rehabilitation technology. This prototype, although an early-stage development, has demonstrated promising capabilities in measuring and recording plantar pressure distribution and dorsiflexion/plantarflexion angles. The innovative use of FSR-embedded insoles and IMU sensors, combined with motor-assisted movement through Bowden cables, showcases the potential for advanced, real-time monitoring and assistance in patient’s rehabilitation. Despite the limitations identified, including sensor inaccuracies, motor control issues, and the current restriction on the number of steps a patient can take due to Bowden cable constraints, the project has laid a solid foundation for future enhancements. The integration of a treadmill and the potential use of myosensors for more effective motor actuation are just a few of the improvements that could significantly enhance the device's functionality and patient outcomes. The prototype's ability to provide real-time data and assistive movement tailored to the patient's effort marks a notable advancement over conventional rehabilitation techniques. The lightweight and wearable design, combined with customizable settings, further underscores the device's practicality and potential for widespread clinical application. In conclusion, while the prototype requires further development and testing, its positive aspects and potential impact on the field of rehabilitation cannot be overstated. With continued research and refinement, this device could revolutionize lower extremity rehabilitation, offering physiotherapists a powerful tool to enhance patient care and outcomes.

## Acknowledgement

This research is self-funded.

## Conflict of interest

The authors confirm that there is no conflict of interest involve with any parties in this research study.

## REFERENCES

[1] Chinn, L., Hertel, J. (2010): Rehabilitation of ankle and foot injuries in athletes. – Clinics in Sports Medicine 29(1): 157-167.

[2] Du Bois, D., Du Bois, E.F. (1916): Clinical calorimetry: tenth paper a formula to estimate the approximate surface area if height and weight be known. – Archives of Internal Medicine 17(6_2): 863-871.

[3] Feng, J., Zhu, F., Li, P., Davari, H., Lee, J. (2021): Development of An Integrated Framework for Cyber-Physical System (CPS)-Enabled Rehabilitation System. – International Journal of Prognostics and Health Management 12(4): 10p.

[4] Ficke, J., Byerly, D.W. (2019): Anatomy, Bony Pelvis and Lower Limb, Foot. – Treasure Island (FL): StatPearls Publishing 10p.

[5] Góes, S.M., Leite, N., Stefanello, J.M., Homann, D., Lynn, S.K., Rodacki, A.L. (2015): Ankle dorsiflexion may play an important role in falls in women with fibromyalgia. – Clinical Biomechanics 30(6): 593-598.

[6] Jette, A.M., Haley, S.M. (2005): Contemporary measurement techniques for rehabilitation outcomes assessment. – Journal of Rehabilitation Medicine 37(6): 339-345.

[7] Kharb, A., Saini, V., Jain, Y.K., Dhiman, S. (2011): A review of gait cycle and its parameters. – IJCEM International Journal of Computational Engineering & Management 13(01): 78-83.

[8] Kim, S., Amjadi, M., Lee, T.I., Jeong, Y., Kwon, D., Kim, M.S., Kim, K., Kim, T.S., Oh, Y.S., Park, I. (2019): Wide range-sensitive, bending-insensitive pressure detection and application to wearable healthcare device. – In 2019 20th International Conference on Solid-State Sensors, Actuators and Microsystems & Eurosensors XXXIII (TRANSDUCERS & EUROSENSORS XXXIII), IEEE 4p.

[9] Li, C., Rusák, Z., Horváth, I., Ji, L., Hou, Y. (2014): Current status of robotic stroke rehabilitation and opportunities for a cyber-physically assisted upper limb stroke rehabilitation. – In Proceedings of TMCE 1: 899-914.

[10] Mawson, S., Nasr, N., Parker, J., Davies, R., Zheng, H., Mountain, G. (2016): A personalized self-management rehabilitation system with an intelligent shoe for stroke survivors: a realist evaluation. – JMIR Rehabilitation and Assistive Technologies 3(1): 12p.

[11] Metsis, V., Jangyodsuk, P., Athitsos, V., Iversen, M., Makedon, F. (2013): Computer aided rehabilitation for patients with rheumatoid arthritis. – In 2013 International Conference on Computing, Networking and Communications (ICNC), IEEE 6p.

[12] Norkin, C.C., White, D.J. (2016): Measurement of joint motion: a guide to goniometry. – FA Davis 591p.

[13] Ohlendorf, D., Kerth, K., Osiander, W., Holzgreve, F., Fräulin, L., Ackermann, H., Groneberg, D.A. (2020): Standard reference values of weight and maximum pressure distribution in healthy adults aged 18-65 years in Germany. – Journal of Physiological Anthropology 39: 1-11.

[14] Orimadegun, A.E., Omisanjo, A.O. (2014): Evaluation of five formulae for estimating body surface area of Nigerian children. – Annals of Medical and Health Sciences Research 4(6): 889-898.

[15] Zhang, W. (2015): Design and Control of a Network-based Gait Rehabilitation System: A Cyber-Physical System Approach. – University of California, Berkeley 113p.